HydRA - Hydrodynamic Response Analysiss

Dual Degree Project Report

Submitted by: **Visharad Jaydas Borsutkar**

Guide: **Dr. Abhilash Somayajula**

Roll no: **NA18B102**

in partial fulfillment of the requirements
for the award of the degree of

MASTER OF TECHNOLOGY

DEPARTMENT OF OCEAN ENGINEERING

INDIAN INSTITUTE OF TECHNOLOGY, MADRAS

April 24, 2023

THESIS CERTIFICATE

This is to certify that the thesis titled **My thesis title**, submitted by **Visharad Jaydas Borsutkar**, to the **Indian Institute of Technology, Madras**, for the award of the degree of **Dual Degree**, is a bona fide record of the research work done by him under my supervision. The contents of this thesis, in whole or in parts, have not been submitted to any other Institute or University for the award of any degree or diploma.

Guide :

Dr. Abhilash Somayajula
Assistant Professor
Department of Ocean Engineering
IIT Madras, 600036

Place: Chennai, TamilNadu 600036
Date: 10 June 2022

TABLE OF CONTENTS

LIST OF TABLES

LIST OF FIGURES

ABSTRACT

Prediction of the dynamic motions of the ship is an essential aspect in the early stages of design as well as later during the service life of the ship. It is crucial to know the motion characteristics of the ship along the six degrees of freedom to operate it safely in adverse sea conditions. The growing number of large ships demands predicting their optimum performance with respect to travel time, fuel efficiency, and the safety of cargo and personnel in specified shipping routes. This can be achieved using efficient and easy-to-use numerical tools capable of predicting hydrodynamics loads on floating vessels with steady forward speed and solving their motion responses in various wave conditions. This project explains the implementation of a three-dimensional potential theory-based program in Python with the consideration of forward speed effects. The theoretical formulation, numerical implementation, and result comparisons are presented in this thesis.

As a part of this dual degree project, a frequency domain 3D panel-based program has been developed and extensively compared against the outputs of MDLHydroD software. KCS and KVLCC2 ship hull forms are analyzed and validated against the MDLHydro software developed by Dr. Amitava Guha. The comparison results are found to be in excellent agreement.

Keywords : Potential theory, Laplace equation, Boundary element method (BEM), Hydrodynamic, Wave structure interaction, Multibody interaction, forward speed, drift force.

CHAPTER 1

INTRODUCTION

1.1 Objective

This Dual Degree project has two main objectives. First is the computation of forces and motion characteristics of a floating body with a zero or non-zero speed in regular waves. A 3D panel-based potential theory method using an infinite-depth green function is used for this computation. The second main objective is the computation of second-order forces for drift force. This software can be used for simple single-body cases and complex multi-body cases. Also, the program's output is validated against industry standard software such as Ansys AQWA and WAMIT v6.

The rest of the thesis is organized as follows. Chapter 1, Introduction, Objective of the project, background and motivation, and a literature review of the research paper used for this project are given. Later, in Chapter 2, the mathematical problem setup and its derivation is given. In Chapter 3, the solution to the numerical mathematical problem is shown, and the motions and forces are computed. Similarly, in Chapter 4, Drift force computation is explained. Later in the subsequent chapter results of the project are compared against Softwares like MDLHydroD and WAMIT6.

1.2 Background and Motivation

A floating body is subjected to various forces, such as environmental loads due to wind, currents, waves, etc. The sea-keeping problem involves calculating the hydrodynamic parameters and forces acting on a floating structure in waves. These hydrodynamic forces are calculated using numerical methods and potential theory for the wave body interaction problem. This can be further used to calculate the RAOs of various vessels.

Hydrodynamic analysis software can help naval architectures optimize the design of vessels in regular waves. It can provide insights into the vessel's performance in various

wave conditions, allowing designers to make informed decisions about the shape and size of the vessel. Also, it saves costs by reducing the need for expensive physical testing. Software for hydrodynamic analysis can allow designers to iterate designs faster, as they can quickly simulate and evaluate the performance of different design configurations. This can help reduce the time-to-market for new vessels and increase productivity.

The primary goal of this project is to develop a flask-based web application named 'HydRA' capable of computing hydrodynamic properties such as Froude Krylov force, scattering force, RAO, radiation damping , and Added Mass for a vessel in zero and non-zero speed scenarios. Also, the implementation of drift forces captures the effect of second-order forces in the deep sea. The main idea behind building an in-house web application is to have a solid foundation for a hydrodynamic analysis tool that can be further improved and extended toward more complex problems. The main reference theses used for this project are Guha and Falzarano (2015), and Guha (2012).

1.3 Literature review

In the early stages of ship design, it is crucial to understand the ship's stability to operate efficiently in the sea. Analyzing a ship's hydrodynamic forces and motion characteristics in regular waves is crucial in designing a stable and safe vessel. With the increase in the availability of computational power, computational fluid dynamics (CFD) has gained popularity in solving fluid-structure interaction problems. However, CFD still takes a significant time to estimate the motion response of floating structures to regular and random waves and is not a viable method during preliminary design. Due to this disadvantage, potential theory-based approaches are still accepted to design floating structures, including offshore oil production platforms, offshore wind turbines, and floating wave energy converters. The strip theory method, which divides a ship into a number of 2D strips along its length, can be credited with the early developments of the potential theory method. The solutions to various two-dimensional problems are combined to determine the three-dimensional hydrodynamics problem. Numerous authors have contributed to this field, including Newman (1979), Ogilvie and Tuck (1969), Beck and Troesch (1990), Journée (2001), Salvesen *et al.* (1970). The work of Salvensen, Tuck, and Faltinsen shown in Salvesen *et al.* (1970) became the widely accepted method that is still employed by the industry for the construction of floating structures. Since the strip theory relies on the slender body assumption, it was not quite applicable to

ship structures and offshore structures, which are non-slender in shape. This led to the development of 3D panel-based potential theory where the floating vessel is discritized into quadrilateral or traingular panels sources of different source strengths. Tuck and Faltinsen 1970 Salvesen *et al.* (1970) provides a detailed review of the theoretical and mathematical models used to predict the motion of ships in waves and the resulting sea loads acting on the hull, which is based on the pressure distribution around the hull and the wave-induced accelerations. The paper covers the effects of ship design parameters, wave steepness and frequency, and wave-induced motions on ship motions. It presents a mathematical model for calculating the sea loads acting on the hull. The paper then discusses the effect of ship design parameters, such as beam and draft, on ship motions and the influence of wave steepness and frequency. The calculation of the Green function efficiently for frequency and time domain analyses has been a long-standing research area. Newman (1979) provides a comprehensive list of methods to compute both frequency domain and time domain Green functions efficiently. Similar work on the zero speed frequency domain Green function has also been reported by Telste and Noblesse (1986). It describes the theoretical background of the green function and the numerical method used to evaluate it.

Guha and Falzarano (2013) and Guha and Falzarano (2015) discuss developing and validating a frequency domain program that uses numerical methods for predicting the motion and hydrodynamic forces acting on floating bodies, specifically ships.

This project documents the theory behind developing an in-house wave analysis tool named 'HydRA' (Hydrodynamic Response Analysis) that can accurately predict the wave loads and motions of a floating structure in various sea conditions. This tool is based on the potential theory of fluid mechanics and uses a numerical method to solve the wave-body interaction problem. The paper provides a detailed description of the theoretical background, numerical implementation, and tool validation. It demonstrates its effectiveness in predicting the wave loads and motions of different floating structures or ships. An in-house tool is developed in this project is to enable the development further to extend it to analyze complex nonlinear hydrodynamic problems such as maneuvering in waves and parametric excitation of ships and offshore structures.

CHAPTER 2

MATHEMATICAL MODEL

In this project, a ship moving with a steady speed of U in deep water with regular waves of wave amplitude A and incident frequency w_I traveling at an angle β with the surge direction of the ship is considered. Potential flow methods are widely used to solve the seakeeping problem. Due to the improvement in the computation power, the three-dimensional boundary element method to compute the wave load can be used.

2.1 Co-ordinate System

In order to set up the mathematical model, two coordinate systems are defined; one of them is the Global coordinate system (GCS), whose origin is located at a calm water level. The other one is the Body seakeeping coordinate system (BCS), whose origin is located at the midship on the intersection of the water line and centerline of the ship. It is further assumed that the x-axis of the GCS points towards the east direction, whereas the x-axis of BCS points towards the sway direction of the ship. Coordinates of points represented in GCS are expressed as $\boldsymbol{x^e} = (x^e, y^e, z^e)$ wheres for the points in BCS it is expressed as $\boldsymbol{x^s} = (x^s, y^s, z^s)$. Global coordinate system, i.e., GCS, denotes the inertial frame of reference. Body geometry and body parameters, such as the location of the vertical center of gravity and radii of gyration, are defined with respect to BSC.

The translating frame of reference i.e. BCS allows the formulation of the vessel response in six degrees of freedom due to incident waves and steady current of speed U in $-x$ direction which is equivalent to forward speed with respect to GCS. A linear boundary value problem can be introduced by assuming a small wave amplitude to determine the velocity potential.

2.2 Velocity potential

Assuming that the fluid flow is inviscid, incompressible, and irrotational the total velocity potential at any point inside the fluid domain is given as :

$$\mathbf{\Phi}(\vec{x},t) = [\,-Ux + \phi_P(\vec{x})\,] + [\,\phi_I(\vec{x},\beta,\omega_I) + \phi_S(\vec{x},\beta,\omega_I) + \sum_{j=1}^{6} n_j\phi_j(\vec{x},U,\omega_e)\,]\,e^{iw_e t} \tag{2.1}$$

In the above equation, ω_I denotes the encounter frequency, ϕ_P represents the perturbation potential due to steady translation, ϕ_I is the incident wave potential, ϕ_S is the scattering wave potential, ϕ_j and n_j are the radiation wave potential due to unit motion and vessel motion amplitude respectively in j^{th} direction. Here, the perturbation potential ϕ_P has a relatively insignificant effect on total potential at low to moderate ship speed. Hence, it will be ignored to reduce the complexity of the problem. Hence, the final equation for velocity potential is given as :

$$\mathbf{\Phi}(\vec{x},t) = -Ux + [\,\phi_I(\vec{x},\beta,\omega_I) + \phi_S(\vec{x},\beta,\omega_I) + \sum_{j=1}^{6} n_j\phi_j(\vec{x},U,\omega_e)\,]\,e^{iw_e t} \tag{2.2}$$

In the above equation, ω_e is the encounter frequency which is expressed in terms of incident or normal wave frequency ω_I , forward speed U, and incident angle β as

$$\omega_e = \omega_I - \frac{\omega_I^2}{g} U\cos\beta \tag{2.3}$$

2.3 Governing equation

The governing equations of the fluid flow are the continuity equation (conservation of mass) and the Navier-stokes equation (conservation of momentum). Under the assumption of inviscid and irrotational flow, the governing equations reduce to Laplace equations given as :

$$\nabla^2(\phi_I,\phi_D,\phi_j) = 0 \tag{2.4}$$

where, ϕ_j $(j = 1, 2, \cdots, 6)$ denotes the radiation potential in all 6-modes of motion. This equation is valid over the entire fluid domain.

2.4 Boundary Conditions

In addition to the governing equation, the velocity potential satisfies the boundary conditions over the fluid boundaries. The total boundary surface S comprises the free surface S_F, mean body surface S_B, bottom surface S_Z, and the radiation surface S_∞ bounding the horizontal infinite fluid domain. The surfaces are shown in Fig. 2.1 below.

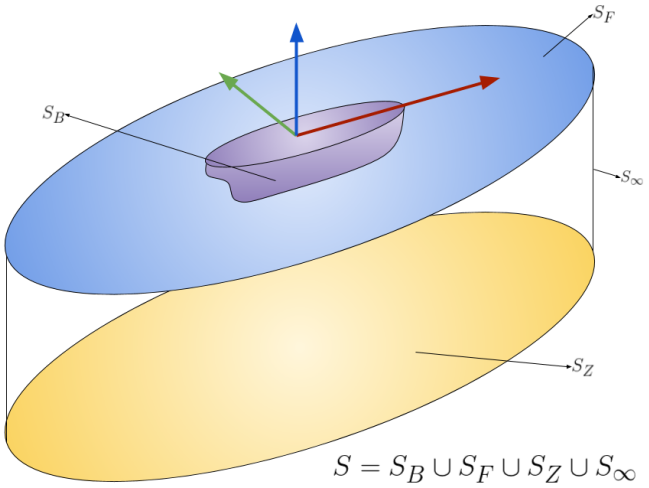

Figure 2.1: Fluid boundary surfaces

The boundary conditions to be satisfied by the potential functions are shown below:

1. Kinematic free surface boundary condition : The velocity of the fluid in the direction normal to the free surface is equal to the velocity of the free surface. If the free surface is given by $z = \eta(t, x, y)$, then the boundary condition is given by

$$\frac{\partial \eta}{\partial t} = \frac{\partial \phi}{\partial z} - \frac{\partial \phi}{\partial x}\frac{\partial \eta}{\partial x} - \frac{\partial \phi}{\partial y}\frac{\partial \eta}{\partial y} \quad \text{over } z \tag{2.5}$$

2. Dynamic free surface boundary condition : The pressure obtained using Bernoulli's equations on the free surface is constant.

$$\left[\left(i\omega_e - u\frac{\partial}{\partial x}\right) + g\frac{\partial}{\partial z}\right](\phi_I, \phi_D, \phi_j) = 0 \quad \text{on } z = 0 \tag{2.6}$$

3. Radiation boundary condition : The waves generated by the oscillating body propagate outward from the body to ∞ in the fluid domain, unbounded horizontally. This boundary condition is also referred to as the Sommerfeld radiation condition.

$$\lim_{kr\to\infty} \sqrt{kr}\left(\frac{\partial}{\partial r} - jk\right)(\phi_j - \phi_I) = 0 \quad \text{for } i = 1, 2, \cdots 6 \tag{2.7}$$

4. Bottom Boundary condition : The normal velocity of the fluid at the bottom boundary is equal to the normal velocity of the boundary. For an impenetrable seabed in deep water, the normal velocity is zero, and the boundary condition is given by

$$\frac{\partial \phi}{\partial z} = 0 \quad \text{over the bottom } z = -\infty \tag{2.8}$$

5. Body surface boundary condition: The velocity of the fluid in the direction normal to the body boundary is equal to the normal velocity of the body boundary over the instantaneous underwater surface S.

$$\frac{\partial \phi_j}{\partial n} = i\omega_e n_j + U m_j \quad \text{on } S \tag{2.9}$$

$$\frac{\partial \phi_I}{\partial n} + \frac{\partial \phi_D}{\partial n} = 0 \quad \text{on } S \tag{2.10}$$

where $\vec{n} = (n_1, n_2, n_3)$ is the unit normal pointing outward from the hull surface and $(n_4, n_5, n_6) = \vec{r} \times \vec{n}$. Here, r is the position vector of a point on the surface. The linear incident wave potential satisfying the above boundary conditions is given by:

$$\phi_I = \frac{igA}{\omega_I} e^{-ik_I(x\cos\beta + y\sin\beta)} e^{kz} \tag{2.11}$$

Here, ω_I represents the incident wave frequency, not the encounter frequency. This forward speed boundary value problem can be solved using potential theory using infinite depth free surface green function.

CHAPTER 3

NUMERICAL SOLUTION

The complex potential on the submerged surface of the vessel is the key to solving the hydrodynamic problem. It will be shown that once the potential is known, all the hydrodynamic coefficients required to obtain all the vessel response, i.e., added mass, damping, and excitation forces, can be calculated.

The boundary value problem described in eq.(2.5) to eq.(2.9) will be solved by a boundary element method. The body surface will be a suitable distribution of source singularities that satisfy the governing equation and the boundary conditions. Solving a Fredholm integral of the second kind over the discretized body boundary will determine the source strengths.

3.1 Integral equation

The velocity potential at some point (x, y, z) in the fluid domain can be expressed in terms of the surface distribution of sources.

$$\phi(\vec{x}) = \frac{1}{4\pi} \int_S \sigma(\vec{x_s}) G(\vec{x} : \vec{x_s})\, dS \tag{3.1}$$

where $\vec{x_s}$ denotes the source point of the body surface, $(\vec{x})$ denotes the point where the potential is being calculated, and $\sigma(\vec{x_s})$ is the unknown source strength distribution on the source point. Section (3.3) will explain the Green function in the upcoming parts. The Green function satisfies the continuity condition and all the boundary conditions, including the free surface and radiation boundary condition, except for the following normal velocity boundary condition on the hull surface:

$$\frac{\partial \phi}{\partial n} = v_n \quad \text{on } S \tag{3.2}$$

Here, $v_n(x, y, x)$ is the flow normal velocity on the hull surface, after applying the velocity boundary condition given in equation (2.2) on the velocity potential (3.1), the below equation is obtained, also known as Fredholm integral of the second kind.

$$-\frac{1}{2}\sigma(\vec{x_s}) + \frac{1}{4\pi}\int_S \sigma(\vec{x_s})\frac{\partial G(\vec{x} : \vec{x_s})}{\partial n} = v_n \quad \text{on } S \tag{3.3}$$

In the above equation, it can be shown that the first term reduces to $-\frac{\sigma}{2}$. Also, $\frac{\partial G}{\partial n}$ denotes the derivative of the Green function in the outward normal direction. This derivative of G can be evaluated from the equation :

$$\frac{\partial G}{\partial n} = \frac{\partial G}{\partial x}n_x + \frac{\partial G}{\partial y}n_y + \frac{\partial G}{\partial z}n_z \tag{3.4}$$

3.2 Numerical Discretization

To solve the eq. (3.3), the body surface is discretized into M panels of area ΔS_m where $m = (1, 2, \cdots, M)$. Every entity presented here is computed at the centroid of the panel. Hence, the source strength as well is computed over each panels centroid. Now, for i^{th} panel eq.(3.3) can be written as:

$$-\frac{1}{2}\sigma_i(\vec{x_s}) + \frac{1}{4\pi}\int_S \sigma_i(\vec{x_s})\frac{\partial G_i(\vec{x} : \vec{x_s})}{\partial n} = v_{n_i} \quad \text{on } S \tag{3.5}$$

Here, the subscript i in the equation represents the entities of an individual panel. While, calculating influence on a panel because of other source panel, the panel where the potential is being calculated and the source panel becomes the same. Due to this, frequency independant part of the green function tends to go to infinity. This case is known as singularity. To compensate for that influence, $-\frac{1}{2}\sigma$ is added into the equation according to the residual theory.

Eq. ()3.5) can be rearranged an written as:

$$-\frac{1}{2}\sigma_i + \frac{1}{2}\sum_{i=1,j=1,i\neq j}^{M} \alpha_{ij}\sigma_i = v_{n_i} \quad \text{for} i = 1, 2, \cdots M \tag{3.6}$$

Here, M is the total number of panels and α represents,

$$\alpha_{ij} = \frac{1}{2\pi} \int_{\Delta S_i} \frac{\partial G(x, x_s)}{\partial n} \, dS \tag{3.7}$$

In physical terms, α_{ij} denotes the velocity induced at the i^{th} panel in the direction normal to the surface by a source distribution of unit strength distributed uniformaly over the j^{th} panel which is the source panel here and i^{th} panel is the influenced panel where the potential is being calculated because of the presence of other source panels.

Now, the eq.(3.6) can be written in the matrix format as :

$$[\sigma] = 2[\alpha - I]^{-1}[v_n] \tag{3.8}$$

where, I represents the unit matrix. $[\alpha]$ is an $m \times m$ cross matrix where m is the total no. of panels. Using the similar adjustments as done in the eq.(3.6), eq.(3.1) can be written as

$$\phi_i = \sum_{j=1}^{m} \beta_{ij} \sigma_j \tag{3.9}$$

All potentials are computed at the centroid of the panels. Now, the above equation can be written in the matrix form as :

$$\{\phi\} = [\beta]\{\sigma\} \tag{3.10}$$

where, $[\beta]$ is the $M \times M$ matrix given by

$$\beta_{ij} = \frac{1}{4\pi} \int_{\Delta S_j} G(\vec{x_i}, \vec{x_s}) dS \tag{3.11}$$

Thus, the boundary problem can be solved for the velocity potential on the body surface if the value of the integral of the Green function G and its derivatives $\frac{\partial G}{\partial n}$ are known.

3.3 Green's Function

For the calculation of radiation and diffraction potential, an infinite-depth green function is used. This Green function and its numerical solution is explained in Telste and Noblesse (1986).

This green function assumes source distribution over the submerged surface of the vessel. It relates the unknown source strength to the velocity potential. Here, the green function comprises two parts: one is the frequency-dependent part, and the other is the frequency-dependent part. The Independent part represents the simple potential and interaction between the body surface and the free surface. On the other hand, the dependent part is to comprise the oscillating potential due to the oscillating source. The equation of the Green function is given as

$$G(\vec{x}, \vec{x_s}, \omega_e) = \frac{1}{r} + \frac{1}{\acute{r}} + \tilde{G}(\vec{x}, \vec{x_s}, \omega_e) \tag{3.12}$$

where,

$$r = ||\boldsymbol{x} - \boldsymbol{x_s}|| = \sqrt{(x - x_s)^2 + (y - y_s)^2 + (z - z_s)^2} \tag{3.13}$$

represents the Eucledian distance between the field point $P(x, y, z)$ and source point $Q(x_s, y_s, z_s)$.

$$r' = \sqrt{(x - \xi)^2 + (y - \eta)^2 + (z + \zeta)^2} \tag{3.14}$$

represents the Euclidean distance between the field point $P(x, y, z)$ and point $Q'(\xi, \eta, \zeta)$, which is the image of the source point in the waterplane $z = 0$ and $\tilde{G}(\vec{x}, \vec{x_s}, \omega_e)$ represents the frequency domain part of the green function, also refree. Note that the frequency used here is the encounter frequency ω_e, shown in the eq. (2.3)

Now, substituting eq.(3.12) in the equations (3.7) and (3.11), gives the following equations for α and β matrices :

$$\alpha_{ij} = -\iint_{\Delta S_i} \frac{\partial}{\partial n}\left(\frac{1}{r}\right) dS - \frac{1}{2\pi}\iint_{\Delta S_j} \frac{\partial}{\partial n}\left(\frac{1}{r'}\right) dS - \frac{1}{2\pi}\iint_{\Delta S_i} \frac{\partial G}{\partial n}(x_i, x_j, \omega_e) dS \tag{3.15}$$

$$\beta_{ij} = -\frac{1}{4\pi}\iint_{\Delta S_i}\left(\frac{1}{r}\right) dS - \frac{1}{4\pi}\iint_{\Delta S_i}\left(\frac{1}{r'} dS\right) - \frac{1}{r}\iint_{\Delta S_i} \tilde{G}(x_i, x_j, \omega_e) dS \tag{3.16}$$

Here, j^{th} panel is the source panel and i_th panel represents the feild point where potential is supposed to be calculated. In the above expressions, first two terms are frequency independant and the last term is frequency dependent which can be obtained by solving for the wavy green function.

3.3.1 Frequency independent part of Green function

The frequency independant part of the α matrix can be computed analytically using the expressions provided by Hess and Smith (1964). Similarly, the frequency independant terms of β matrix can be evaluated using the expressions given by Katz and Plotkin (2001). Expressions used to get all the frequency independant terms as mentioned below.

Now, normal derivatives can be expressed as the sum of dot products of normal unit vectors and the partial derivatives in x, y and z directions. Hence,

$$\iint_{\Delta S_i} \frac{\partial}{\partial n}\left(\frac{1}{r}\right) dS = n_x \iint_{\Delta S_m} \frac{\partial}{\partial n}\left(\frac{1}{r}\right) dS + n_y \iint_{\Delta S_i} \frac{\partial}{\partial n}\left(\frac{1}{r}\right) dS \tag{3.17}$$

$$+ n_z \iint_{\Delta S_i} \frac{\partial}{\partial n}\left(\frac{1}{r}\right) dS \tag{3.18}$$

Now, equations for the partial derivatives required to compute the normal derivative are given below :

$$\begin{aligned}\iint_{\Delta S_m} \frac{\partial}{\partial x}\left(\frac{1}{r}\right) dS = &\frac{y_2 - y_1}{d_{12}} \ln\left(\frac{r_1 + r_2 - d_{12}}{r_1 + r_2 + d_{12}}\right) \\ &+ \frac{y_3 - y_2}{d_{23}} \ln\left(\frac{r_2 + r_3 - d_{23}}{r_2 + r_3 + d_{23}}\right) \\ &+ \frac{y_4 - y_3}{d_{34}} \ln\left(\frac{r_3 + r_4 - d_{34}}{r_3 + r_4 + d_{34}}\right) \\ &+ \frac{y_1 - y_4}{d_{41}} \ln\left(\frac{r_4 + r_1 - d_{41}}{r_4 + r_1 + d_{41}}\right)\end{aligned} \tag{3.19}$$

$$\begin{aligned}\iint_{\Delta S_m} \frac{\partial}{\partial y}\left(\frac{1}{r}\right) dS = &\frac{x_1 - x_2}{d_{12}} \ln\left(\frac{r_1 + r_2 - d_{12}}{r_1 + r_2 + d_{12}}\right) \\ &+ \frac{x_2 - x_3}{d_{23}} \ln\left(\frac{r_2 + r_3 - d_{23}}{r_2 + r_3 + d_{23}}\right) \\ &+ \frac{x_3 - x_4}{d_{34}} \ln\left(\frac{r_3 + r_4 - d_{34}}{r_3 + r_4 + d_{34}}\right) \\ &+ \frac{x_4 - x_1}{d_{41}} \ln\left(\frac{r_4 + r_1 - d_{41}}{r_4 + r_1 + d_{41}}\right)\end{aligned} \tag{3.20}$$

$$\begin{aligned}\iint_{\Delta S_m} \frac{\partial}{\partial z}\left(\frac{1}{r}\right) dS = &\tan^{-1}\left(\frac{m_{12}e_1 - h_1}{zr_1}\right) - \tan^{-1}\left(\frac{m_{12}e_2 - h_2}{zr_2}\right) \\ &+ \tan^{-1}\left(\frac{m_{23}e_2 - h_2}{zr_2}\right) - \tan^{-1}\left(\frac{m_{23}e_3 - h_3}{zr_3}\right) \\ &+ \tan^{-1}\left(\frac{m_{34}e_3 - h_3}{zr_3}\right) - \tan^{-1}\left(\frac{m_{34}e_4 - h_4}{zr_4}\right) \\ &+ \tan^{-1}\left(\frac{m_{41}e_4 - h_4}{zr_4}\right) - \tan^{-1}\left(\frac{m_{41}e_4 - h_1}{zr_1}\right)\end{aligned} \tag{3.21}$$

Similarly, the frequency dependent part of the $[\beta]$ matrix is given by

$$\begin{aligned}\iint_{\Delta S_m} \left(\frac{1}{r}\right) dS = &\left[\frac{(x-x_1)(y_2-y_1) - (y-y_1)(x_2-x_1)}{d_{12}} \ln\left(\frac{r_1+r_2+d_{12}}{r_1+r_2-d_{12}}\right)\right. \\ &+ \frac{(x-x_2)(y_3-y_2) - (y-y_2)(x_3-x_2)}{d_{23}} \ln\left(\frac{r_2+r_3+d_{23}}{r_2+r_3-d_{23}}\right) \\ &+ \frac{(x-x_3)(y_4-y_3) - (y-y_4)(x_4-x_3)}{d_{34}} \ln\left(\frac{r_3+r_4+d_{34}}{r_3+r_4-d_{34}}\right) \\ &\left.+ \frac{(x-x_4)(y_1-y_4) - (y-y_4)(x_1-x_4)}{d_{41}} \ln\left(\frac{r_4+r_1+d_{41}}{r_4+r_1-d_{41}}\right)\right] \\ &- z\left[\tan^{-1}\left(\frac{m_{12}e_1 - h_1}{zr_1}\right) - \tan^{-1}\left(\frac{m_{12}e_2 - h_2}{zr_2}\right)\right. \\ &+ \tan^{-1}\left(\frac{m_{23}e_2 - h_2}{zr_2}\right) - \tan^{-1}\left(\frac{m_{23}e_3 - h_3}{zr_3}\right) \\ &+ \tan^{-1}\left(\frac{m_{34}e_3 - h_3}{zr_3}\right) - \tan^{-1}\left(\frac{m_{34}e_4 - h_4}{zr_4}\right) \\ &\left.+ \tan^{-1}\left(\frac{m_{41}e_4 - h_4}{zr_4}\right) - \tan^{-1}\left(\frac{m_{41}e_1 - h_1}{zr_1}\right)\right]\end{aligned} \tag{3.22}$$

In the above expression, instead of $|z|$ as reported in Katz and Plotkin (2001), only z is used. This modifies expression is found to be in good agree with the point source approximation as the distance between the field panel and source panel increases.

In the above expressions (3.19), (3.20), (3.21) and (3.22) the intermediate terms are

given by the below equations:

$$d_{12} = \sqrt{(x_2 - x_1)^2 + (y_2 - y_1)^2} \tag{3.23}$$
$$d_{23} = \sqrt{(x_3 - x_2)^2 + (y_3 - y_2)^2} \tag{3.24}$$
$$d_{34} = \sqrt{(x_4 - x_3)^2 + (y_4 - y_3)^2} \tag{3.25}$$
$$d_{41} = \sqrt{(x_1 - x_4)^2 + (y_1 - y_4)^2} \tag{3.26}$$

$$m_{12} = \frac{y_2 - y_1}{x_2 - x_1} \tag{3.27}$$
$$m_{23} = \frac{y_3 - y_2}{x_3 - x_2} \tag{3.28}$$
$$m_{34} = \frac{y_4 - y_3}{x_4 - x_3} \tag{3.29}$$
$$m_{41} = \frac{y_1 - y_4}{x_1 - x_4} \tag{3.30}$$

$$r_1 = \sqrt{(x - x_1)^2 + (y - y_1)^2 + z^2} \tag{3.31}$$
$$r_2 = \sqrt{(x - x_2)^2 + (y - y_2)^2 + z^2} \tag{3.32}$$
$$r_3 = \sqrt{(x - x_3)^2 + (y - y_3)^2 + z^2} \tag{3.33}$$
$$r_4 = \sqrt{(x - x_4)^2 + (y - y_4)^2 + z^2} \tag{3.34}$$

$$e_1 = z^2 + (x - x_1)^2 \tag{3.35}$$
$$e_2 = z^2 + (x - x_2)^2 \tag{3.36}$$
$$e_3 = z^2 + (x - x_3)^2 \tag{3.37}$$
$$e_4 = z^2 + (x - x_4)^2 \tag{3.38}$$

3.3.2 Frequency dependent part of Green function

The frequency dependent part of the integrals of the green function which is $\tilde{G}(x, x_s, \omega_e)$ and its derivatives are evaluated using the numerical methods given in Telste and No-

blesse (1986). The given expressions for derivatives and integrals are shown below :

$$\tilde{G}(\boldsymbol{x}, \boldsymbol{x_s}, \omega_e) = 2f\left[R_0(h,v) - i\pi J_0(h)e^v\right] \tag{3.39}$$

$$\frac{\partial \tilde{G}_0}{\partial \rho_G} = -2f^2\left[R_1(h,v) - i\pi J_1(h)e^v\right] \tag{3.40}$$

$$\frac{\partial \tilde{G}_0}{\partial x} = \frac{(x_P^e - x_Q^e)}{\rho_G}\frac{\partial \tilde{G}_0}{\partial \rho_G} \tag{3.41}$$

$$\frac{\partial \tilde{G}_0}{\partial y} = \frac{(y_P^e - y_Q^e)}{\rho_G}\frac{\partial \tilde{G}_0}{\partial \rho_G} \tag{3.42}$$

$$\frac{\partial \tilde{G}_0}{\partial z} = 2f^2\left[\frac{1}{d} + R_0(h,v) - i\pi J_0(h)e^v\right] \tag{3.43}$$

where,

$$f = \frac{\omega^2 L}{g} \tag{3.44}$$

$$\rho_G = \left[(x_P^e - x_Q^e)^2 + (y_P^e - y_Q^e)^2\right]^{\frac{1}{2}} \tag{3.45}$$

$$r = \left[\rho_G^2 + (z_P^e - z_Q^e)^2\right]^{\frac{1}{2}} \tag{3.46}$$

$$r' = \left[\rho_G^2 + (z_P^e + z_Q^e)^2\right]^{\frac{1}{2}} \tag{3.47}$$

$$h = f\rho_G \tag{3.48}$$

$$v = f(z_P^e + z_Q^e) \tag{3.49}$$

$$d = fr' \tag{3.50}$$

J_0 and J_1 are the first-kind Bessel functions, L is a non-dimensionalizing length selected by the user, and g is the acceleration brought on by gravity. This study makes use of $L = 1$. Real valued functions $R_0(h,v)$ and $R_1(h,v)$ are effectively evaluated using the numerical method suggested by Telste and Noblesse (1986).

Once, the potentials are computed ,pressure can be obtained on each panel. Through integration of pressure throughout the submerged surface forces can be evaluated. Using radiation potentials added mass and radiation damping can be computed. After, obtaining all these coeffecients and using them motion equation can be solved to get the RAOs. Steps to compute these forces and motion are explained in detail in the next section.

CHAPTER 4

FORCES and MOTIONS

something something one para

4.1 Wave Potentials

how to compute force

4.2 Exciting forces

4.3 Forward speed RAO

CHAPTER 5

DRIFT FORCES

5.1 Problem statement

5.2 Numerical solution

CHAPTER 6

RESULTS AND DISCUSSION

The outputs of the program are compared against the output of the software MDLHydroD. The devlopment of the MDLHydroD software is explained in Guha and Falzarano (2013) and Guha and Falzarano (2015). For comparison KCS and KVLCC2 vessels are considered.

6.1 KCS Vessel

KCS is a fine form container ship and its particulars are listed in Table 6.2. For comparison, frequencies are used from -0.03 with $+0.03$ increment, in totoal 34 frequencies are used. Ship's speed is $8\,\mathrm{m\,s^{-1}}$. Incident angles used ranges from $0°$ to $345°$ with $15°$ increment. Simulation is ran for 6 modes of motion. The comparison of added mass for different angles are shown in figure 6.1 and figure 6.1. Comparisons of radiation damping is shown in figure 2. Comparisons of Froude Krylov force is shown in figure 2. Comparisons of Scattering force is shown in figure 2. Comparisons of RAO is shown in figure 2.

Table 6.1: KCS principal particulars

Main Particulars	**Value**
Length between perpendiculars $L\ (m)$	230
Breadth $B\ (m)$	32.2
Draft $d\ (m)$	10.8
Displacement $\nabla\ (m^3)$	52030
Block coefficient C_b	0.651
Radius of Gyration R_{zz}/L	0.25
Metacentric height $GM\ (m)$	1.20
LCB (% of L from midship, forward +ve)	-1.48%

6.1.1 Added Mass

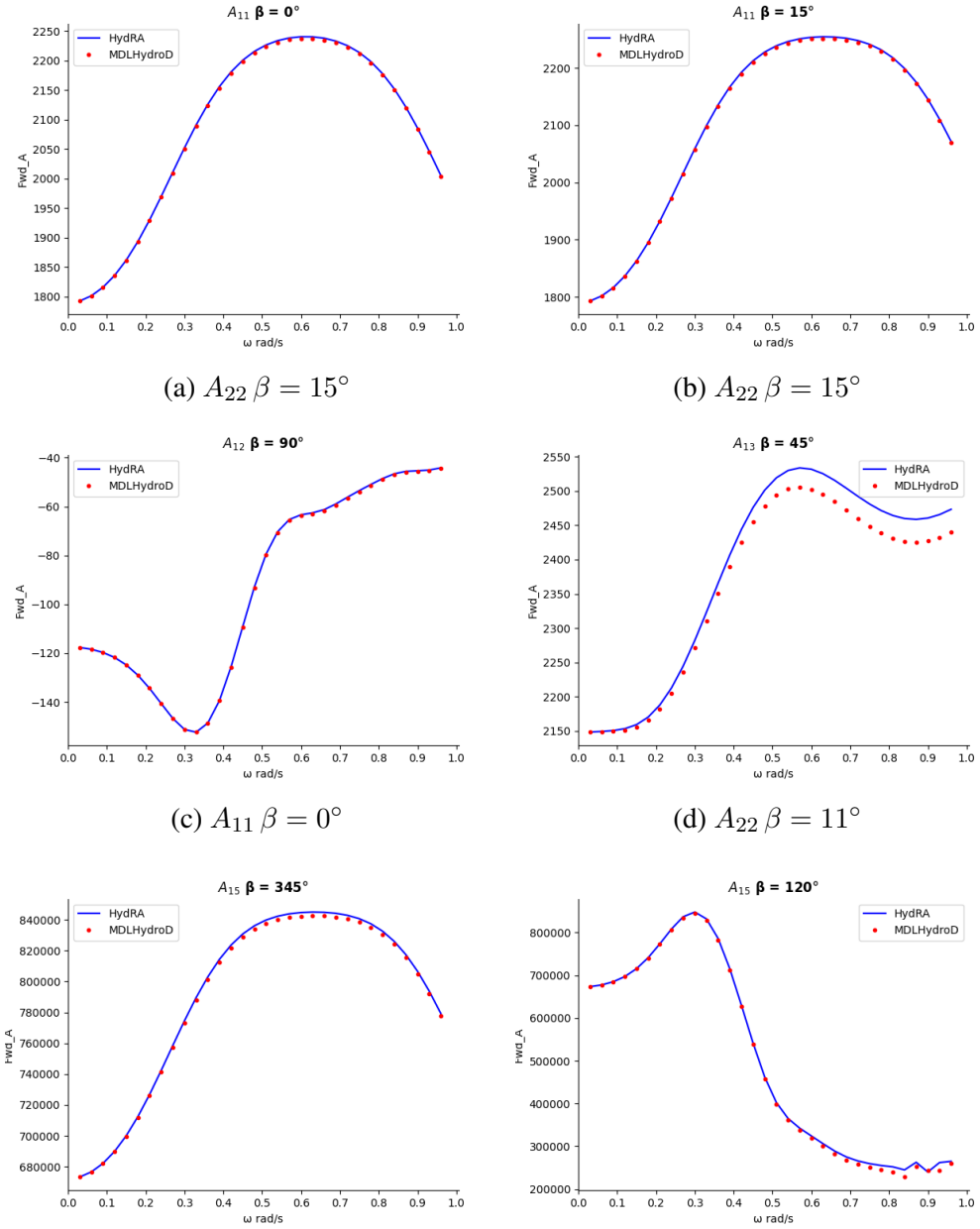

(a) A_{22} $\beta = 15°$

(b) A_{22} $\beta = 15°$

(c) A_{11} $\beta = 0°$

(d) A_{22} $\beta = 11°$

(e) A_{22} $\beta = 12°$

(f) A_{22} $\beta = 13°$

Figure 6.1: KCS vessel added mass comparison - I

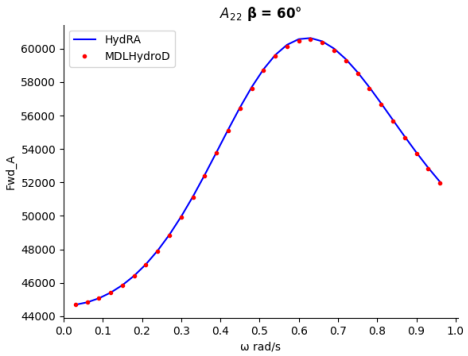

(g) $A_{22}\ \beta = 14°$

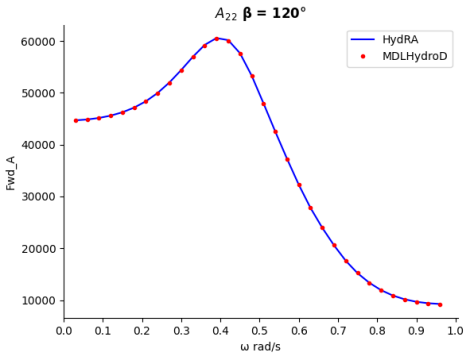

(h) $A_{22}\ \beta = 15°$

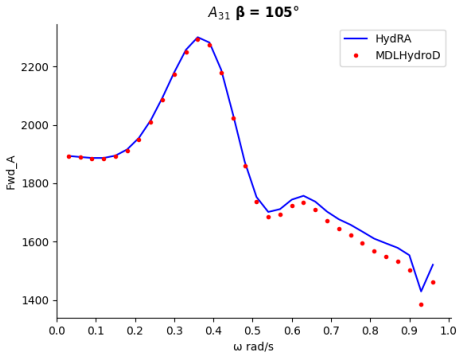

(i) $A_{22}\ \beta = 16°$

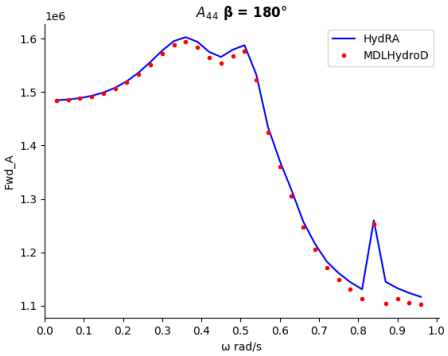

(j) $A_{22}\ \beta = 17°$

Figure 6.1: KCS vessel added mass comparison - II

6.1.2 Radiation Damping

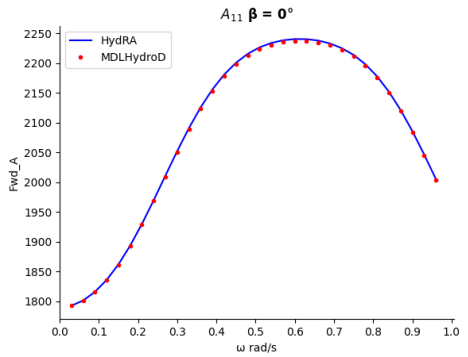

(a) $A_{11}\ \beta = 0°$

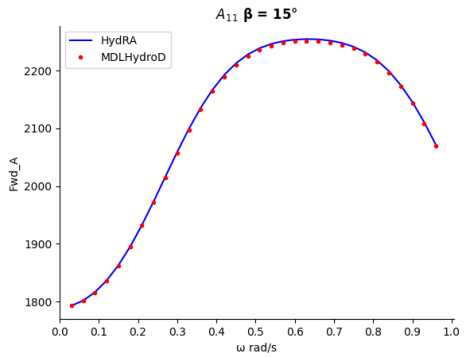

(b) $A_{22}\ \beta = 15°$

6.1.3 Froude Krylov Force

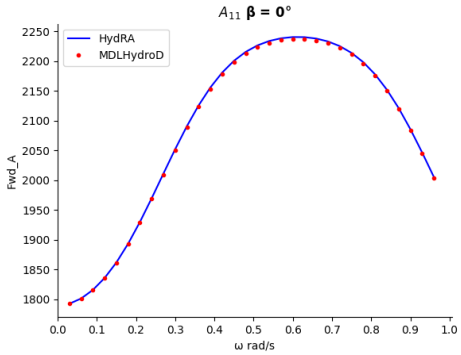

(a) A_{11} $\beta = 0°$

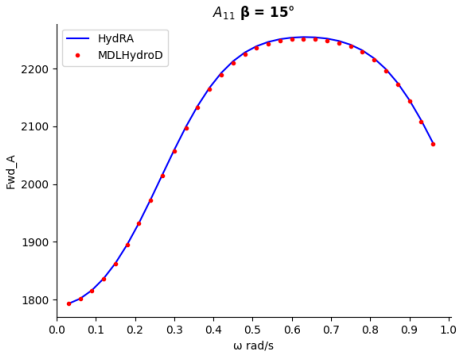

(b) A_{22} $\beta = 15°$

6.1.4 Scattering Force

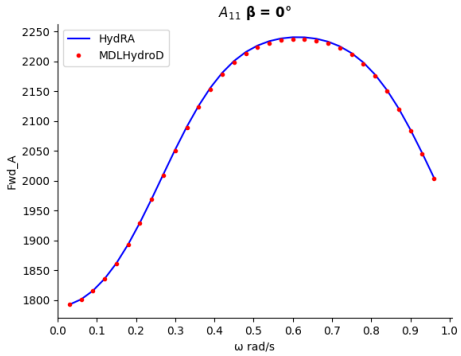

(a) A_{11} $\beta = 0°$

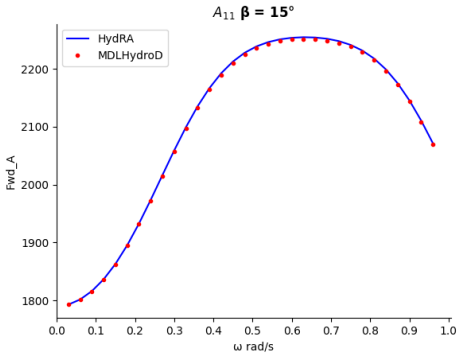

(b) A_{22} $\beta = 15°$

6.2 KVLCC Vessel

Input parameters for KVLCC2 are given in the following table.

parameter	value
something	something
something	something

Table 6.2: Parameters KCS vessel

CHAPTER 7

CONCLUSION

A new numerical web-based frequency domain tool is developed to compute hydrodynamic force and motions with low to moderate forward speed. The effect of forward speed is included using the encountering frequency and the changing boundary conditions.

REFERENCES

1. **Beck, R. F.** and **A. W. Troesch** (1990). Documentation and user's manual for the computer program shipmo. *Department of Naval Architecture and Marine Engineering, The University of Michigan*.

2. **Guha, A.** (2012). *Development of a computer program for three dimensional frequency domain analysis of zero speed first order wave body interaction*. Ph.D. thesis.

3. **Guha, A.** and **J. Falzarano**, Development of a computer program for three dimensional analysis of zero speed first order wave body interaction in frequency domain. *In International Conference on Offshore Mechanics and Arctic Engineering*, volume 55393. American Society of Mechanical Engineers, 2013.

4. **Guha, A.** and **J. Falzarano** (2015). Estimation of hydrodynamic forces and motion of ships with steady forward speed. *International Shipbuilding Progress*, **62**(3-4), 113–138.

5. **Hess, J. L.** and **A. M. O. Smith** (1964). Calculation of nonlifting potential flow about arbitrary three-dimensional bodies. *Journal of ship research*, **8**(04), 22–44.

6. **Journée, J.** (2001). Theoretical manual of seaway. *Delft University of Technology Shiphydromechanics Laboratory,(Release 4.19, 12-02-2001), http://www. shipmotions. nl/DUT/PapersReports/1370-StripTheory-03. pdf*.

7. **Katz, J.** and **A. Plotkin**, *Low-speed aerodynamics*, volume 13. Cambridge university press, 2001.

8. **Newman, J. N.** (1979). The theory of ship motions. *Advances in applied mechanics*, **18**, 221–283.

9. **Ogilvie, T. F.** and **E. O. Tuck** (1969). A rational strip theory of ship motions: part i. Technical report, University of Michigan.

10. **Salvesen, N.**, **E. Tuck**, and **O. Faltinsen** (1970). Ship motions and sea loads.

11. **Telste, J.** and **F. Noblesse** (1986). Numerical evaluation of the green function of water-wave radiation and diffraction. *Journal of Ship Research*, **30**(02), 69–84.